EUROPEAN FUSION DEVELOPMENT AGREEMENT

EFDA–JET–PR(05)01/08

J.S. deGrassie, L-G Eriksson, J-M Noterdaeme and JET-EFDA contributors

Toroidal Rotation and ICRF Heating in NBI-Driven Discharges in JET

Toroidal Rotation and ICRF Heating in NBI-Driven Discharges in JET

J.S. deGrassie[1], L-G Eriksson[2], J-M Noterdaeme[3] and JET EFDA Contributors*

[1]General Atomics, P.O. Box 85608, San Diego, California, 92186-5608 USA †Association
[2]EURATOM/CEA Cadarache F-13108 St-Paul-Lez-Durance, France
[3]Max-Planck IPP-EURATOM Association, Boltzmann-Str. 2, D-85748, Garching, Germany and University Gent, EESA Department, Gent, Belgium
**See annex of J. Pamela et al, "Overview of JET Results",*
(Proc.20 [th] IAEA Fusion Energy Conference, Vilamoura, Portugal (2004).

Preprint of Paper to be submitted for publication in Proceedings of the
16th Topical Conference on Radio Frequency Power in Plasmas
(Utah, USA, 11-13 April 2005)

ABSTRACT.
The addition of RF heating to an NBI-driven target discharge is observed to reduce the toroidal rotation frequency. Experiments on this effect were performed on JET using (H)-D and (^{3}He)-D minority ICRH to vary the bulk electron to ion heating ratio. However, to lowest order, there is no clear difference in the two heating scenarios. We apply a recent model of Nishijima et al. based upon the degradation of confinement with auxiliary power, and find that these JET data are in reasonable agreement with it.

In general, the application of rf heating to a tokamak discharge with an established toroidal rotation driven by Neutral Beam Injection (NBI) results in a reduction of the magnitude of this rotation [1–4]. One explanation is that the additional heating power increases the turbulent transport of toroidal momentum [2–4]. Ion temperature gradient turbulence is predicted to be enhanced with greater T_e/T_i, the electron to ion temperature ratio, and this would appear to qualitatively fit with DIII–D experiments in which direct-electron rf heating is applied [1–3].

A series of experiments has been performed on JET designed to test the effect of T_e/T_i upon this reduction in toroidal speed by utilizing two different minority ICRH scenarios in order to vary the ratio of bulk electron to bulk ion heating [5]. In bulk ion D discharges, the standard JET minority H ICRH results in strong electron heating. The other scenario selected is minority ^{3}He with the object of reducing the electron heating in favor of bulk ion heating. Post-experiment modeling with the PION code [6] indicates that this was only partially successful. The change in T_e/T_i was not large, and the basic response of the plasma rotation to added ICRH appears insensitive to the heating scenario used, to lowest order. There may be subtle profile differences, but these cannot be definitively extracted from the data.

Since enhanced auxiliary heating with added ICRH is the common factor in either JET scenario, we will test the recent model of Nishijima et al. [4] used to explain a similar slowing observed in ASDEX-U. Briefly, this model postulates a decrease in energy and toroidal momentum confinement times (assumed to be equal) as $1/\sqrt{P_{aux}}$, where P_{aux} is the total auxiliary heating power. Incrementally, added P_{rf} increases P_{aux} but does not supply any significant toroidal torque, so there is an incremental decrease in the momentum confinement time and, hence, momentum itself. But P_{rf} does supply heating power, so there is a net gain in total energy.

The set of data from these JET sessions includes both L– and H–mode discharges, and target discharges with co- and counter-NBI, relative to the direction of toroidal plasma current. All have $B_T = 3.4$T, and $I_p = 1.8$MA. For the (H) heating scenario f = 51MHz, launched on the four-strap antennas with 0 0 $\pi\pi$ phasing, while for (^{3}He) f = 33 MHz with 0π0π phasing. The phasing difference is due to technical reasons. In each case, the fundamental resonance passes near the magnetic axis, R ~ 3.0m.

A typical toroidal rotation response in the JET co-NBI, L–mode discharges is shown in Fig.1. Two shots are displayed, one for each ICRH scenario. In Fig.1(a) we show T_i near the core ($\rho \cong 0.17$), the toroidal rotation frequency, ω_ϕ, at the same location, and the rf power profile, P_{rf}, while in Fig.1(b) are T_e ($\rho \cong 0.17$), n_{e1}, the line-averaged electron density, and the NBI power, P_{NBI}. The clear signature

of a reduction in ω_ϕ is seen with application of P_{rf}, recovering after the RF pulse. In contrast, the thermal energies, indicated by the temperatures, rise steadily throughout the RF pulse. There is an indication of greater T_i at this location for the (^{3}He) discharge. It appears that there is a small increase in the thermal confinement time throughout the shot since the temperatures return to a higher value after the rf pulse than before, at the same PNBI. This is also indicated by the return of ω_ϕ to a slightly larger value, on average.

In Fig.1 we have divided ω_ϕ by the factor of 8.3 determined by a computation of the NBI torque to power ratio, as described in Ref. [3]. If this scaled value of ω_ϕ were equal to T_i, then the $\tau_{\phi i}$ parameter, defined in Ref. [3], would be 1, as generally seen in the core in DIII–D. Here in JET, this parameter is about twice this value for these discharges.

We will evaluate the dataset in terms of the ASDEX model [4]. The global (volume integrated) toroidal angular momentum, L, and thermal energy, W , are described by

$$\begin{aligned} L &= N\tau = s\, P_{NBI}\, \tau \\ W &= P\tau = (P_{NBI} + P_{NBI})\ \tau \quad , \end{aligned} \tag{1}$$

where τ is a common confinement time for both. This model neglects the ohmic heating power as small. The beam injected torque is N and the ratio of N to P_{NBI} is s, nominally equal to $2R_{tan}/V_b$, where R_{tan} is the beam trajectory tangency major radius and V_b is the beam particle speed. The confinement time is modeled to decay with auxiliary power as $\tau = C/\sqrt{P}$, where C is a constant for fixed target discharge conditions. So W increases with P_{rf} as $W = C\,(P_{rf} + P_{NBI})^{1/2}$, while L decreases with P_{rf} as $L = C_s P_{NBI}\ /P_{rf} + P_{NBI})^{1/2}$. L and W are computed from the data by doing the volume integrals of the mechanical momentum density, $n_i M_i R^2\ \omega_\phi$, and energy density, $(3/2)(n_i T_i + n_e T_e)$, respectively. Here we assume that the ion density n_i is equal to n_e, and that ω_ϕ, T_e, T_i, and n_e are flux functions, and we replace R^2 in the L integral by R_0^2, where R_0 is the major radius of the magnetic axis.

In Fig.2(a) we plot the time histories of W and L for the same two discharges as in Fig.1. Both show an increase in these global quantities with rf power, in spite of the core reduction in ω_ϕ seen in Fig.1(a). Note that the value of s for the JET NBI mix in these two discharges is s s =1μs = 1 Nt-m-s/MJ, and we see then from Fig.2(a) that the global confinement times of W and L are indeed very similar. Figure 2(b) shows 0.5s averaged values of W and L scaled to their initial (averaged) value prior to rf turn-on, plotted versus $1+P_{rf}/P_{NBI}$. Although L/L_1 does increase with P_{rf}, this increase is much less than that seen in W/W_1 with P_{rf}. We conclude that qualitatively the ASDEX model predicts the difference in response of W and L with P_{rf}, but here there is an overall bias toward an increase in each, which is probably due to an increase in τ throughout the discharge, that is, C = C(t). After the rf pulse, W clearly returns to a value above the starting value, at the same NBI power, and this is seen to a lesser extent in L, as shown in Fig.2(b).

In order to apply the ASDEX model to this entire dataset of JET discharges we define a parameter, A, by taking the ratio of L to W , as defined above. That is,

$$A = \left[\left(P_{NBI} + P_{rf}\right)/s\, P_{NBI}\right](L/W) = \left[\left(1 + P_{rf}/P_{NBI}\right)/s\right](L/W), \tag{2}$$

motivated by the discussion following Eq. (1). This serves to remove C from each discharge and leaves only the power dependence of τ. In computing A for a discharge, we compute the actual, possibly time dependent, value of s given the NB injectors used for the specific discharge. The data is time-averaged for 0.25s to generate a data point. The ASDEX model predicts A = 1 for all values of P_{rf}/P_{NBI}. Actually, in Ref. [4] this model is applied only to changes due to RF within a discharge and does not require the conclusion that L /Ws = in a steady NBI-only portion of a discharge.

The resultant values of A for 22 discharges, taken in three separate sessions spanning nearly two years, are shown in Fig.3, where we plot A versus $1 + P_{rf}/P_{NBI}$. Each session falls clearly into its own band of points, with A relatively independent of P_{rf}/P_{NBI}, again supporting the Nishijima et al. explanation of the reduction in L with P_{rf} [4].

The cause of the separate bands of points is revealed by the set of data taken with counter-NBI, the lowest values of A. As is well-known, a tokamak has nonzero L even with $P_{NBI} = 0$, that is, there is an 'intrinsic' rotation, L_0, which is not negligible [7–10]. L_0 is typically in the direction of I_p, but it can be opposite. For the counter discharges, it is observed that there is an L_0, which would be negative if shown in Fig.3 because it is in the direction of Ip, opposite to the direction of toroidal NBI in this case. (L is positive in the direction of toroidal NBI in Fig.3.) In one discharge, the early NBI rotation data indicates that $L_0 \sim -0.25$ Nt-m-s near the start of the rf pulse. Thus, L and W should be replaced in Eq. (1) by $L - L_0$ and $W - W_0$, where W_0 would logically be the Ohmic heating energy. This would raise the A values for the counter-NBI discharges by ΔA, $0.15 < \Delta A < 0.35$. There are also L_0 values, now positive, for the other data in Fig. 3, which would lower A for these sets. Care must be taken to purposely measure L_0 with short NBI pulses. Including the fact that $L_0 = L_0$ (W) [7,10] also complicates the details of applying the ASDEX model, although its basic plausibility is consistent with these JET results.

ACKNOWLEDGMENT

Work supported in part by the U.S. Department of Energy under Contract DEFC02-04ER54698.

REFERENCES

[1]. J.S. deGrassie et al., Proc. 13th Top. Conf. on RF Power in Plasmas, Annapolis (1999) p. 140.

[2]. J.S. deGrassie et al., Proc. 26th EPS Conf. on Contr. Fusion and Plasma Phys., Maastricht, Vol. 23J, 1189 (1999).

[3]. J.S. deGrassie et al., Nucl. Fusion **43**, 142 (2003).

[4]. D. Nishijima et al., Plasma Phys. Control. Fusion, **47**, 89 (2005).

[5]. V.P. Bhatnagar et al., Nucl. Fusion **33**, 83 (1993).

[6]. L.-G. Eriksson and T. Hellsten, Phys. Scr., **55**, 70 (1995).

[7]. J.E. Rice et al., Phys. Plasmas **11**, 2427 (2004), and references therein.

[8]. L.-G. Eriksson, E. Righi, and K.-D. Zastrow, Plasma Phys. Control. Fusion, **39**, 27 (1997).

[9]. J.-M. Noterdaeme et al., Nucl. Fusion **43**, 274 (2003).

[10]. J.S. deGrassie et al., Phys. Plasmas **11**, 4323 (2004).

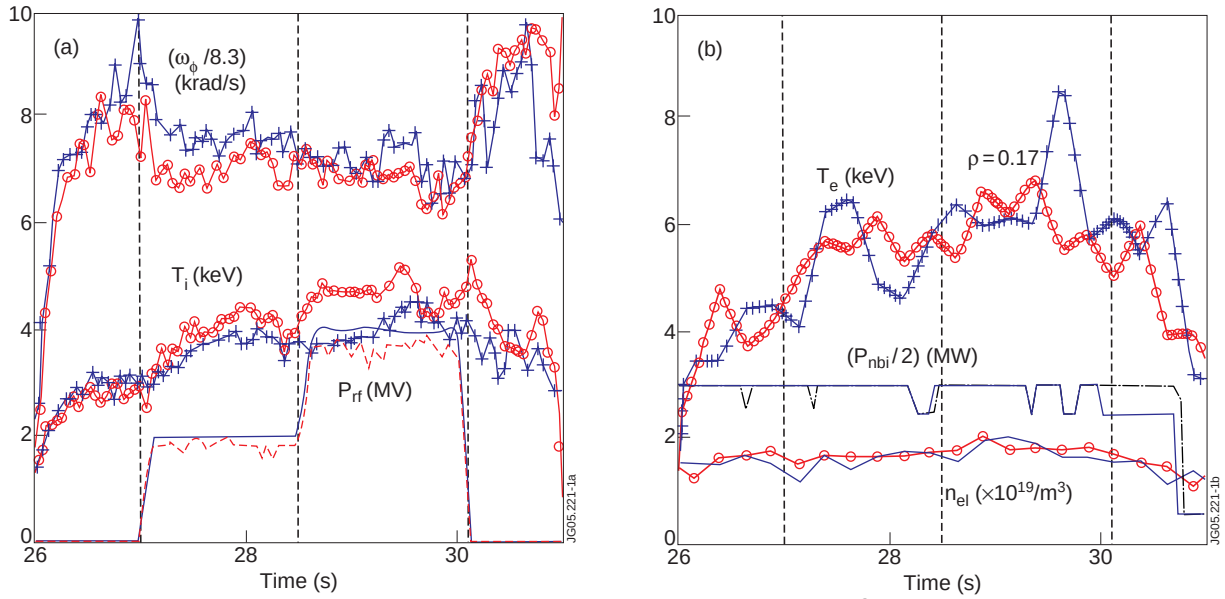

Figure 1: (a) ω_ϕ, T_i, and P_{rf} versus time. (H)-D Pulse No: 55664 N(+, - - -) and (^{3}He)-D Pulse No: 55666 (o ,—) (b) T_e, n_{e1}, and P_{NBI}.

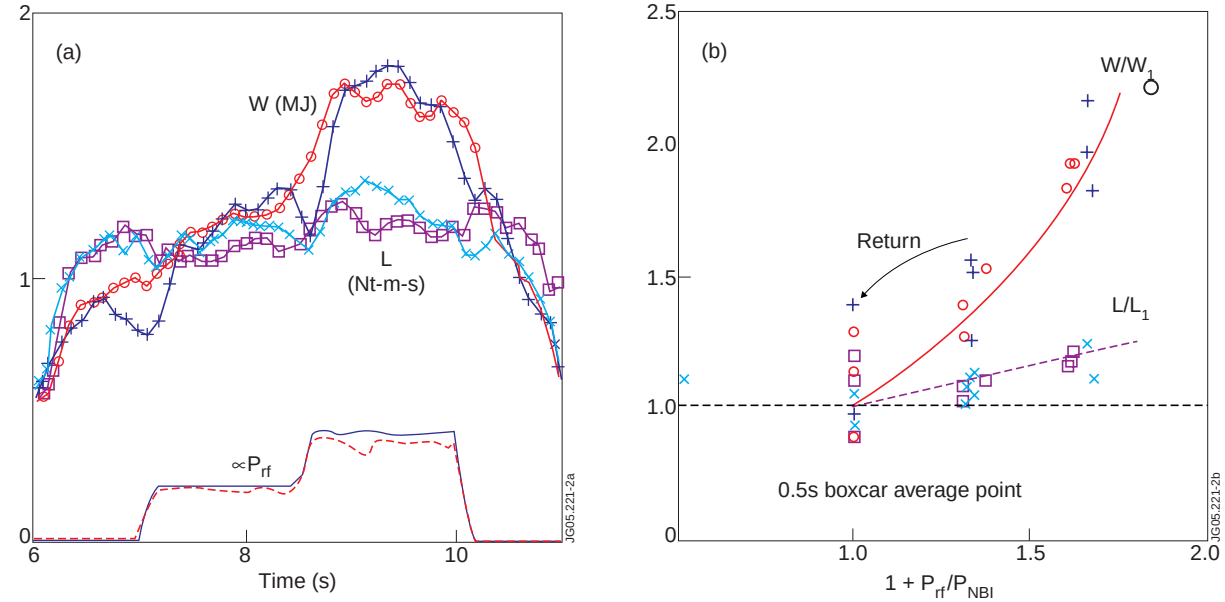

Figure 2: (a) Volume integrated thermal energy, W, and toroidal mechanical angular momentum, L, versus time. (H)-D (+, ×), (^{3}He)-D (○ ,□). (b) W and L scaled to values with P_{NBI} only, prior to P_{rf}, versus 1+P_{rf} /P_{NBI}.

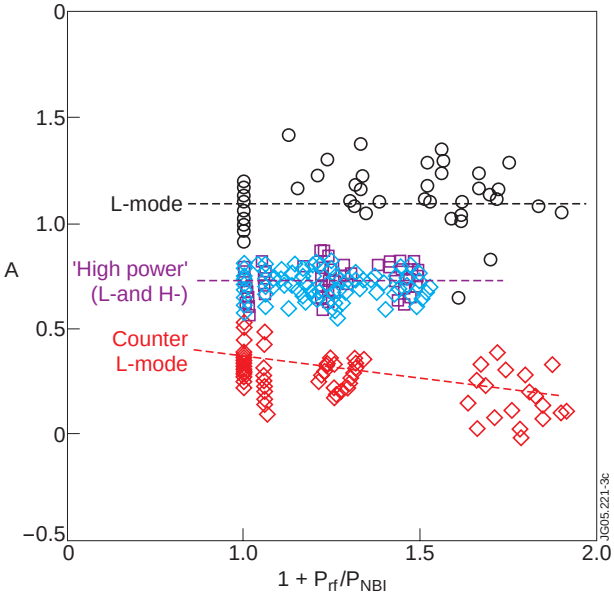

Figure 3: Parameter ' A' versus 1+P_{rf} /P_{NBI}. 'L–mode' consists of 4 co-NBI pulses. 'High-power' consists of 12 co-NBI pulses with some L– and H–mode cases. 'Counter' consists of 6 counter-NBI pulses in L–mode. The data points are 0.25s boxcar averages in a pulse.